https://doi.org/10.1016/j.optlaseng.2019.05.011

Single-shot in-line holographic authentication using phase and amplitude modulation

Wen Chen[1,2,*]

[1]Department of Electronic and Information Engineering, The Hong Kong Polytechnic University, Hong Kong, China

[2]The Hong Kong Polytechnic University Shenzhen Research Institute, Shenzhen 518057, China

**Email: owen.chen@polyu.edu.hk*

Abstract

In this paper, single-shot in-line holographic authentication using phase and amplitude modulation is presented. Amplitude modulation and phase modulation are presented and conducted at reference wave path to obtain noise-like reference wavefront and to generate the parameters (masks) at reference wave path as security keys for single-shot in-line digital holography, and its application, i.e., optical authentication, is presented to show validity of the proposed digital holographic system. A reference optical path using the cascaded random amplitude-only and phase-only masks is applied as an example. Only one in-line digital hologram is used for object reconstruction, and the recovered objects can be effectively authenticated. It is illustrated that parameters (e.g., masks) flexibly designed at reference wave path can facilitate wavefront retrieval in the CCD plane and also can act like security keys for optical information authentication. @ Elsevier, 2019.

Keywords: Optical security; Single-shot holography; Optical authentication; In-line holographic authentication

1. Introduction

Due to rapid development of modern technologies, digital holography [1,2] has attracted much attention in various applications, such as microscopy [3], optical security [4] and optical metrology [5]. Digital holography can record the whole field information related to a sample, and object reconstruction can be conducted by using numerical approaches without wet-chemical processing.

Until now, there are several types of digital holographic setups, such as off-axis [1,6], in-line [7] and parallel [8,9]. In the off-axis digital holography, a small angle between object wave and reference wave is used to generate spatial carrier for separating zero order term and twin image [1,6,10]. However, off-axis digital holographic setup is limited by low-resolution detectors, and space bandwidth is not high. In the in-line digital holography, phase-shifting algorithm [5,7] is commonly applied to extract object wavefront and is able to overcome inherent problem in the off-axis digital holography by using several exposures with phase shifts at reference wave path. However, much experimental effort should be made, and phase-shifting setup is not highly suitable for dynamic measurements. Recently, it has been found that parallel phase-shifting digital holography [8,9] can provide a new alternative. However, some devices (such as pixelated optical items) should be precisely aligned in the holographic setup, and optical components should be carefully fabricated. Single-exposure phase-shifting digital holography [11] has been developed as an effective method to overcome the above problems, and complex-valued object wavefront in the CCD plane can be extracted for the reconstruction. However, the recovered object is of very low quality, and its potential applications, e.g., optical authentication and security [12–19], have not been explored.

In this paper, single-shot in-line holographic authentication using phase and amplitude modulation is presented. Amplitude modulation and phase modulation are presented and conducted at reference wave path for single-shot in-line digital holography, and its application, i.e., optical information authentication, is further explored and presented to show validity of the proposed method. A reference optical path using the cascaded random amplitude-only and phase-only masks is applied as an example. Only one in-line digital hologram is used for object reconstruction, and the recovered objects can be effectively authenticated. It is illustrated that parameters (masks) flexibly designed at reference wave path can facilitate wavefront retrieval in the CCD plane and also can act like security keys for optical authentication.

2. Principles

Figure 1 shows a schematic setup for the proposed digital holography authentication method. A collimated plane wave is generated, and is divided by a beam splitter cube into object beam and reference beam. At the object wave path, object wavefront in the CCD plane can be described by [20]

$$O(\mu,\nu)=\frac{j}{\lambda}\int_{-\infty}^{+\infty}\int_{-\infty}^{+\infty}O(x,y)\frac{1}{\rho}\exp\left(-j\frac{2\pi}{\lambda}\rho\right)dxdy, \tag{1}$$

where $O(\mu,\nu)$ denotes object wavefront in the CCD plane, (μ,ν) denotes coordinate of the CCD plane, $O(x,y)$ denotes the test object, λ denotes light wavelength, ρ denotes the distance from a point in the object plane to a point in the CCD plane $\rho=\sqrt{(x-\mu)^2+(y-\nu)^2+d^2}$, $j=\sqrt{-1}$, and d denotes axial distance. Here, the free-space wave propagation process is implemented by [20]

$$O(\mu,\nu)=O(x,y)\otimes\Im(x,y,d), \tag{2}$$

where $\otimes$ stands for the convolution, and $\Im(x, y, d)$ denotes point pulse function of the Fresnel transform described by

$$\Im(x, y, d) = \frac{\exp(j2\pi d/\lambda)}{jd\lambda} \exp\left[\frac{j\pi}{d\lambda}(x^2 + y^2)\right]. \tag{3}$$

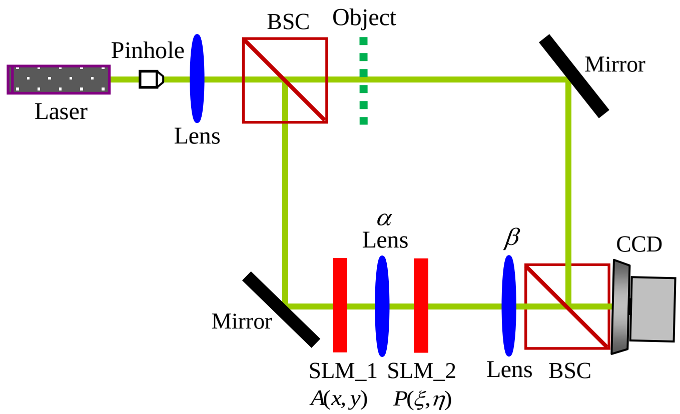

Fig. 1. A schematic setup for the proposed method: BSC, beam splitter cube; CCD, charge-coupled device; SLM, spatial light modulator. Random amplitude-only mask is embedded into SLM_1, and random phase-only mask is embedded into SLM_2. In practice, these two SLMs can be placed in the optical setup to reflect the propagating beam, i.e., reflective. Cascaded-mask optical arrangement is applied at reference wave path, however it is straightforward to design other optical structures for the generation of noise-like reference wavefront in the CCD plane and the control of parameters or masks (acting like security keys) at reference wave path.

At the reference wave path, optical components can be flexibly applied, and random amplitude-only and phase-only masks are cascaded and used as a typical example. Fractional Fourier transform (FrFT) [21] is employed at reference wave path. Hence, reference wavefront in the CCD plane can be described by

$$R(\mu, \nu) = \mathrm{FrFT}_{\beta,\beta}\left(\left\{\mathrm{FrFT}_{\alpha,\alpha}\left[A(x, y)\right]\right\} P(\xi, \eta)\right), \tag{4}$$

where $A(x, y)$ denotes random amplitude-only mask, $P(\xi, \eta)$ denotes random phase-only mask, and α and β denote FrFT function orders. The one-dimensional FrFT can be described by [21]

$$\mathrm{FrFT}_{\alpha}\left[A(x)\right] = \int_{-\infty}^{+\infty} A(x)\, T_{\alpha}(\xi_{\alpha}, x)\, dx, \tag{5}$$

where $T_\alpha(\xi_\alpha, x) = \begin{cases} W\exp\left\{ j\pi\left[\xi_\alpha^2 \cot\left(\alpha\pi/2\right) + x^2 \cot\left(\alpha\pi/2\right) - 2\xi_\alpha x \csc\left(\alpha\pi/2\right) \right] \right\} & \text{if } \alpha \neq 2m \\ \delta(\xi_\alpha - x) & \text{if } \alpha = 4m \\ \delta(\xi_\alpha + x) & \text{if } \alpha = 4m \pm 2 \end{cases}$, m denotes an integer, and $W = \sqrt{1 - j\cot\left(\alpha\pi/2\right)}$.

An in-line digital hologram $I(\mu, \nu)$ formed by using interference principle is recorded by CCD camera, and is expressed by

$$I(\mu,\nu) = \left[O(\mu,\nu) + R(\mu,\nu) \right]\left[O(\mu,\nu) + R(\mu,\nu) \right]^*, \tag{6}$$

where asterisk denotes complex conjugate.

In this study, the proposed digital holographic method is applied for information authentication, and random amplitude-only and phase-only masks $A(x, y)$ and $P(\xi, \eta)$ at the designed reference wave path act like security keys. When these keys and setup parameters are available to the authorized person, reference wavefront in the CCD plane can be first calculated, i.e., $\hat{R}(\mu,\nu) = \mathrm{FrFT}_{\beta,\beta}\left(\left\{\mathrm{FrFT}_{\alpha,\alpha}\left[A(x, y)\right]\right\} P(\xi,\eta)\right)$. Subsequently, extraction of complex-valued object wavefront in the CCD plane consists of the following steps:

(i) Four neighboring pixels in the digital hologram, i.e., $I(k,l)$, $I(k,l+1)$, $I(k+1,l)$ and $I(k+1,l+1)$, are categorized as one group, and are respectively re-denoted as $I1$, $I2$, $I3$ and $I4$.

(ii) The corresponding four neighboring pixels of the extracted reference wavefront $\hat{R}(\mu,\nu)$ are also considered as one group. These four pixels are respectively denoted as $t1\exp(j\varphi1)$, $t2\exp(j\varphi2)$, $t3\exp(j\varphi3)$ and $t4\exp(j\varphi4)$, where $t1-t4$ denote amplitude parts and $\varphi1-\varphi4$ denote phase parts.

(iii) To simplify the retrieval computation, it is assumed that the corresponding four neighboring pixels of object wavefront are the same, i.e., $t0\exp(j\varphi0)$.

(iv) After the above conditions in steps (i)–(iii) are set, the four neighboring pixels of object wavefront can be extracted by using a method similar to phase-shifting algorithm [5,7,11,22], which is described by

$$t0 = \frac{\sqrt{Q1+Q2}}{2\left(Z1-Z2\right)}, \tag{7}$$

$$\varphi0 = \tan^{-1}\left[\frac{\breve{I}\left(t1\cos\varphi1 - t2\cos\varphi2\right) - \hat{I}\left(t3\cos\varphi3 - t4\cos\varphi4\right)}{\hat{I}\left(t3\sin\varphi3 - t4\sin\varphi4\right) - \breve{I}\left(t1\sin\varphi1 - t2\sin\varphi2\right)} \right], \tag{8}$$

where the symbols [11,22] are respectively described by

$$Q1 = \left[\hat{I}\left(t3\sin\varphi3 - t4\sin\varphi4\right) - \breve{I}\left(t1\sin\varphi1 - t2\sin\varphi2\right) \right]^2,$$

$$Q2 = \left[\breve{I}\left(t1\cos\varphi1 - t2\cos\varphi2\right) - \hat{I}\left(t3\cos\varphi3 - t4\cos\varphi4\right) \right]^2,$$

$$\hat{I} = I1 - I2 - (t1^2 - t2^2),$$

$$\breve{I} = I3 - I4 - (t3^2 - t4^2),$$

$$Z1 = \left(t1\cos\varphi1 - t2\cos\varphi2\right)\left(t3\sin\varphi3 - t4\sin\varphi4\right),$$

$$Z2 = \left(t1\sin\varphi1 - t2\sin\varphi2\right)\left(t3\cos\varphi3 - t4\cos\varphi4\right).$$

(v) Similarly, other groups (i.e., each group with four neighboring pixels) in the digital hologram can also be processed, hence object wavefront $\hat{O}(\mu,\nu)$ [i.e., $t0\exp(j\varphi 0)$] in the CCD plane can be extracted. Subsequently, amplitude part of the extracted object wavefront $\hat{O}(\mu,\nu)$ is further processed by using a median filter with a window of 3×3 pixels to generate a filtered complex-valued object wavefront $\hat{O}_f(\mu,\nu)$. Finally, the test object can be reconstructed by using free-space wave back-propagation principle described by

$$\hat{O}(x,y) = \hat{O}_f(\mu,\nu) \otimes \Im(\mu,\nu,-d), \tag{9}$$

where $\hat{O}(x,y)$ denotes a recovered object. Since only one in-line digital hologram is available for the recovery and grayscale object (normalized) is studied, the recovered object cannot visually render useful information. Here, correlation coefficient (CC) and mean squared error (MSE) are calculated to describe quality of recovered objects, and optical information authentication is conducted to verify the recovered object by using nonlinear correlation algorithm [23–37].

$$\begin{aligned} N(x,y) = \Bigg| \mathrm{IFT}\Bigg(\Big| \{\mathrm{FT}[O(x,y)]\}\{\mathrm{FT}[\hat{O}(x,y)]\}^* \Big|^{\nu-1} \\ \times \{\mathrm{FT}[O(x,y)]\}\{\mathrm{FT}[\hat{O}(x,y)]\}^* \Bigg) \Bigg|^2, \end{aligned} \tag{10}$$

where $N(x,y)$ denotes an authentication distribution, ν denotes the strength of applied nonlinearity (i.e., 0.30), and FT and IFT denote Fourier transform and inverse Fourier transform, respectively. Original images can be separately stored [24,26], and only a platform interface is available to authorized persons without disclosure of original object information. The application objective in this study is to verify the recovered object image without visually observing original object information, i.e., acting as a novel optical security strategy. It can be considered that an additional security layer is established over optical encryption [4,13,35,38–40]. A flow chart is shown in Fig. 2 to clearly illustrate the proposed method aforementioned.

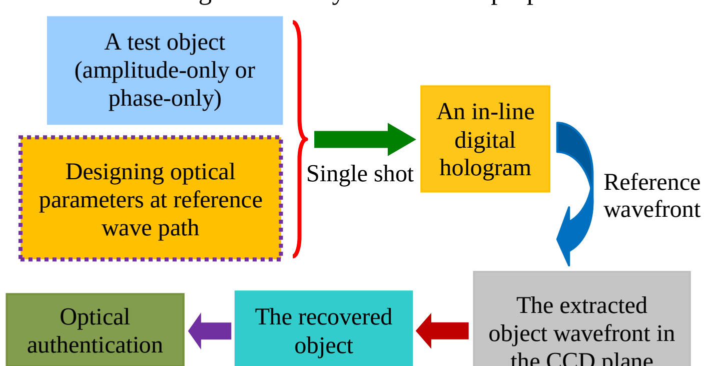

Fig. 2. A flow chart for optical authentication using the proposed digital holographic method.

3. Results and discussion

The setup shown in Fig. 1 is applied to numerically illustrate validity of the proposed method, and the data are processed to generate the decryption and authentication results. The plane wave (wavelength of 632.8 nm) is used, and is divided by a beam splitter cube into reference wave and object wave. At object wave path, axial distance between the object and the CCD plane is 13.0 cm. At reference wave path, a random amplitude-only mask can be embedded into the first spatial light modulator, and a random phase-only mask can be embedded into the second spatial light modulator. The amplitude-only mask is randomly distributed in a range of [0, 200], and the phase-only mask is randomly distributed in a range of $[0, 2\pi]$. In practice, the value range for amplitude-only mask can be flexibly designed to satisfy different applications. The FrFT function orders α and β are 0.80 and 0.50, respectively. Figures 3(a) and 3(b) show amplitude and phase parts of complex-valued reference wavefront in the CCD plane, respectively. Since random masks are placed at the designed reference wave path, noise-like reference wavefront is generated. In this study, in-line digital holography is applied, and only one digital hologram is obtained (such as by using CCD camera with pixel size of $4.65\,\mu\text{m}$ and pixel number of 512×512) as shown in Fig. 3(c). In practice, the proposed method can be flexibly carried out by using optical or virtual-optics approach. For instance, SLMs can be placed in the optical setup to embed the masks and reflect the propagating beam at reference wave path, such as a reflective arrangement.

An image with 512×512 pixels, i.e., "Baboon" (http://sipi.usc.edu/database), is normalized as the test object to show validity of the proposed method. Figure 4(a) shows a recovered object, when all parameters in the proposed optical system are correctly applied. CC and MSE for Fig. 4(a) are 0.10 and 0.71, respectively. It can be seen in Fig. 4(a) that the recovered object cannot visually render object information. In this study, nonlinear correlation algorithm [23–37] is applied to authenticate the recovered object, and the corresponding authentication distribution is shown in Fig. 4(b). It is illustrated that the recovered object is correctly verified, since only one remarkable peak is generated at the center of the authentication distribution. System robustness is further tested, when the recorded hologram is contaminated. Figure 4(c) shows a recovered object, when 128×128 pixels of the hologram are occluded (i.e., set as zeros). CC and MSE for Fig. 4(c) are 0.098 and 0.64, respectively. Figure 4(d) shows an authentication distribution corresponding to Fig. 4(c). Figure 4(e) shows a recovered object, when the hologram is contaminated by additive white noise (zero mean noise with variance of 3). CC and MSE for Fig. 4(e) are 0.095 and 0.72, respectively. Figure 4(f) shows an authentication distribution corresponding to Fig. 4(e). It is illustrated in Figs. 4(d) and 4(f) that the proposed method possesses high robustness against the contaminations.

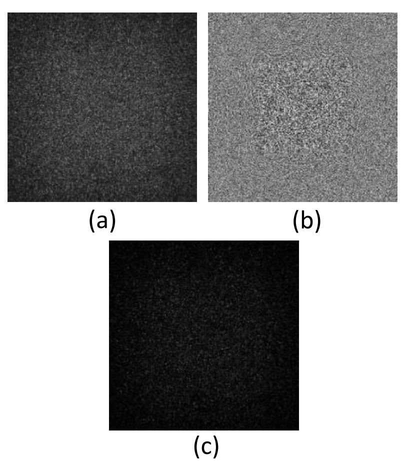

Fig. 3. (a) Amplitude part and (b) phase part of complex-valued reference wavefront in the CCD plane, and (c) an in-line digital hologram.

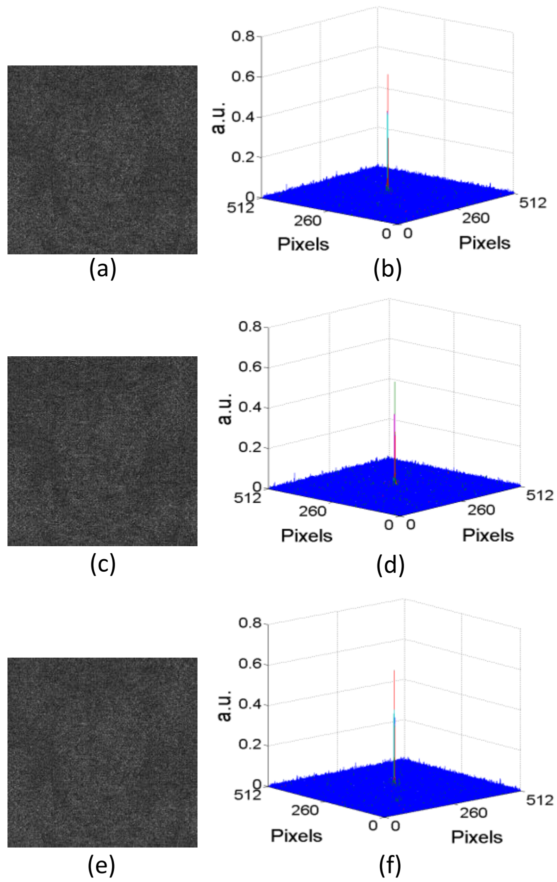

Fig. 4. (a) A recovered object obtained when all parameters in the proposed optical system are correctly applied, (b) an authentication distribution corresponding to (a); (c) a recovered object obtained when 128×128 pixels of the hologram are occluded, (d) an authentication distribution corresponding to (c); (e) a recovered object obtained when the hologram is contaminated by additive white noise, (f) an authentication distribution corresponding to (e).

The cascaded random amplitude-only and phase-only masks are used at reference wave path, however it is straightforward to design other optical structures to generate noise-like reference wavefront in the CCD plane. This flexibility at reference wave path makes the proposed optical authentication system secure, since parameters designed at the reference wave path can act like security keys. It should be emphasized that main contribution of this study is to design complex parameters at reference wave path as security keys and apply only one in-line digital hologram for optical authentication. Figure 5(a) shows a recovered object, when amplitude-only mask is wrongly used to generate reference wave. Figure 5(b) shows an authentication distribution corresponding to Fig. 5(a). Figure 5(c) shows a recovered object, when phase-only mask is wrongly used to generate reference wave. Figure 5(d) shows an authentication distribution corresponding to Fig. 5(c). It can be seen in Figs. 5(b) and 5(d) that only noisy correlation distributions are obtained, when the designed parameters at reference wave path are wrongly used for the recovery. In this case, the wrong amplitude-only mask or wrong phase-only mask is defined as those also randomly generated within the designed ranges. Other parameters, such as FrFT function orders, can be considered as complementary keys. Figure 5(e) shows a recovered object, when only FrFT function order α contains an error of 0.01 during the generation of reference wave for the reconstruction. Figure 5(f) shows an authentication distribution corresponding to Fig. 5(e). It is worth noting that the parameters and masks used at reference wave path, such as distance (or FrFT function orders) and amplitude-only or phase-only mask, can perform like principal security keys for the proposed digital holographic authentication.

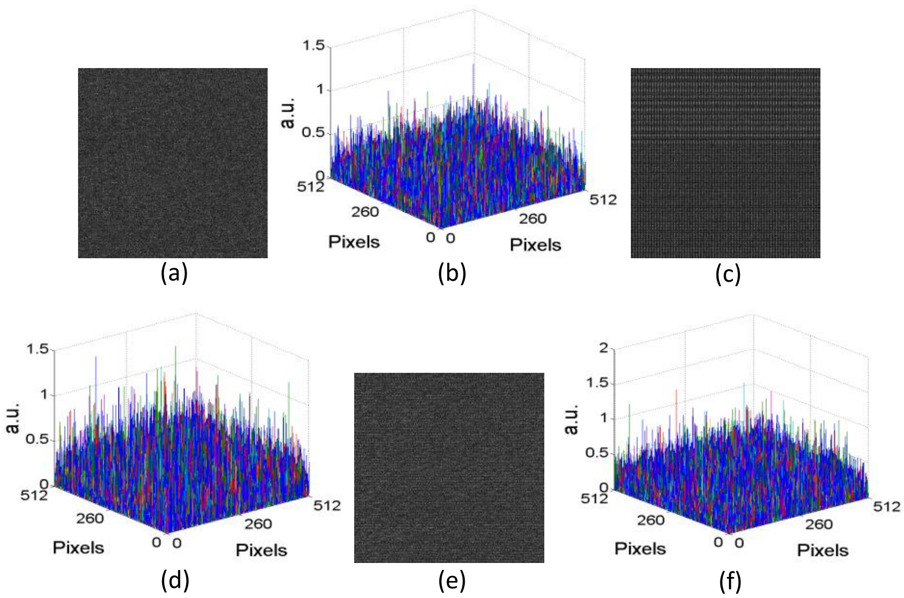

Fig. 5. (a) A recovered object obtained when amplitude-only mask is wrongly used to generate reference wave, (b) an authentication distribution corresponding to (a); (c) A recovered object obtained when phase-only mask is wrongly used, (d) an authentication distribution corresponding to (c); (e) A recovered object obtained when only FrFT function order α contains an error of 0.01, (f) an authentication distribution corresponding to (e). The CC values for (a), (c) and (e) are 0.00025, -0.0048 and -0.0015, respectively. The MSE values for (a), (c) and (e) are 7.1×10^4, 3.8×10^5 and 1.6×10^5, respectively.

In practice, the test object can be sparsified before the recording, and some pixels of the object image can be set as zeros to enhance invisibility of the recovered objects. It is found that the recovered objects can still be verified by using the proposed method. Figure 6(a) shows a recovered object, when all parameters in the proposed optical system are correctly applied. 2.0% pixels of the object image, i.e., 5242 pixels, are set as zeros before hologram recording. CC and MSE for Fig. 6(a) are 0.088 and 0.77, respectively. Figure 6(b) shows an authentication distribution corresponding to Fig. 6(a). Figure 6(c) shows a recovered object, when all parameters in the proposed optical system are correctly applied. In this case, 5.0% pixels of the object image, i.e., 13107 pixels, are set as zeros before hologram recording. CC and MSE for Fig. 6(c) are 0.066 and 0.99, respectively. Figure 6(d) shows an authentication distribution corresponding to Fig. 6(c). It can be seen in Figs. 6(b) and 6(d) that the recovered objects can still be effectively verified, when the object image is compressed before the recording.

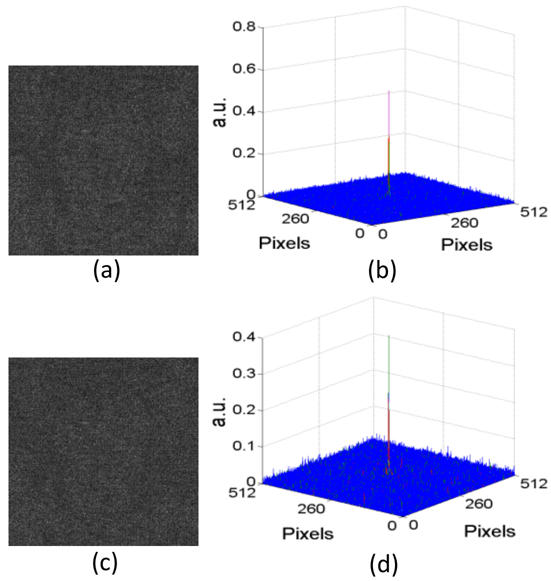

Fig. 6. (a) A recovered object obtained when all parameters in the proposed optical system are correctly applied and 2.0% pixels of the object image are set as zeros before hologram recording, (b) an authentication distribution corresponding to (a); (c) A recovered object obtained when all parameters in the proposed optical system are correctly applied and 5.0% pixels of the object image are set as zeros before hologram recording, (d) an authentication distribution corresponding to (c).

In Figs. 4–6, amplitude-only image is used as the test object, and a phase object can also be verified based on the proposed digital holographic system. Figure 7(a) shows a recovered phase object, when all parameters in the designed optical system are correctly applied. In this case, 35.0% pixels of the object image are set as zeros before converting to phase object for the recording, and other setup parameters are the same as those for Fig. 4(a). CC and MSE for Fig. 7(a) are 0.069 and 2.57, respectively. It can be seen in Fig. 7(a) that the recovered phase object does not visually provide clear information. The corresponding authentication distribution is shown in Fig. 7(b). It can be seen in Fig. 7(b) that optical information authentication can still be correctly conducted. Figure 7(c) shows a recovered phase object, when 128×128 pixels of the hologram are occluded (i.e., set as zeros). Figure 7(d) shows an authentication distribution corresponding to Fig. 7(c). Figure 7(e) shows a recovered phase object, when the hologram is contaminated by additive white noise (zero mean noise with variance of 3). Figure 7(f) shows an authentication distribution corresponding to Fig. 7(e). It is illustrated in Figs. 7(d) and 7(f) that when phase object is studied, the proposed method still possesses high robustness against the contaminations.

Performance of the designed parameters at reference wave path is further evaluated. Figure 8(a) shows a recovered phase object, when amplitude-only mask is wrongly used to generate reference wave. Figure 8(b) shows an authentication distribution corresponding to Fig. 8(a). Figure 8(c) shows a recovered phase object, when phase-only mask is wrongly used to generate reference wave. Figure 8(d) shows an authentication distribution corresponding to Fig. 8(c). It can be seen in Figs. 8(b) and 8(d) that only noisy correlation outputs are obtained, when the designed parameters at reference wave path are wrongly used. Figure 8(e) shows a recovered phase object, when only FrFT function order α contains an error of 0.01 for the generation of reference wave during object reconstruction. Figure 8(f) shows an authentication distribution corresponding to Fig. 8(e).

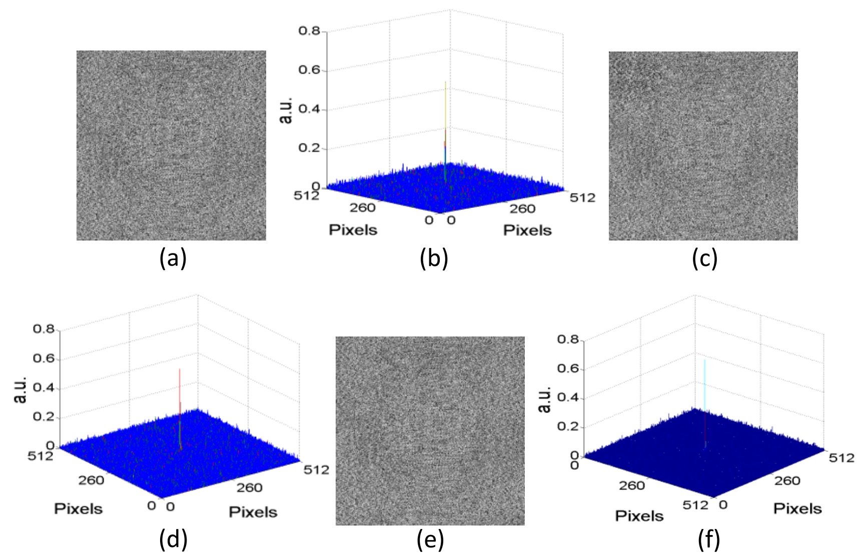

Fig. 7. Phase object case: (a) a recovered phase object obtained when all parameters in the proposed optical system are correctly applied, (b) an authentication distribution corresponding to (a); (c) a recovered phase object obtained when 128×128 pixels of the hologram are occluded, (d) an authentication distribution corresponding to (c); (e) a recovered phase object obtained when the hologram is contaminated by additive white noise, (f) an authentication distribution corresponding to (e). The CC values for (c) and (e) are 0.069 and 0.070, respectively. The MSE values for (c) and (e) are 2.62 and 2.57, respectively.

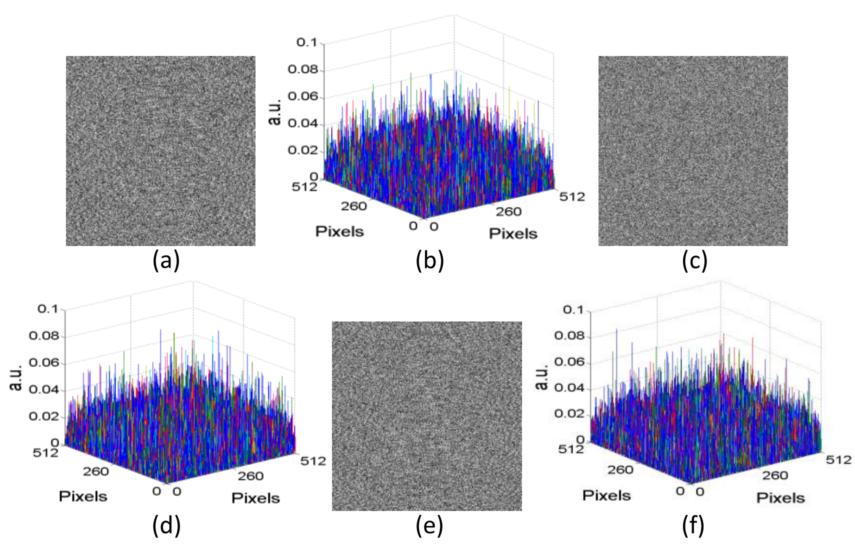

Fig. 8. Phase object case: (a) a recovered phase object obtained when amplitude-only mask is wrongly used to generate reference wave, (b) authentication distribution corresponding to (a); (c) A recovered phase object obtained when phase-only mask is wrongly used to generate reference wave, (d) authentication distribution corresponding to (c); (e) A recovered phase object obtained when only FrFT function order α contains an error of 0.01 for the generation of reference wave, (f) authentication distribution corresponding to (e). The CC values for (a), (c) and (e) are 0.00047, -0.00012 and 0.0015, respectively. The MSE values for (a), (c) and (e) are 3.96, 3.95 and 3.94, respectively.

4. Conclusions

Amplitude and phase modulation has been presented and conducted at reference wave path for single-shot in-line digital holography, and its application, i.e., optical information authentication, has been developed. Reference wave path is designed to generate different parameters as security keys, and only one in-line digital hologram is used for object reconstruction. The results demonstrate that the recovered objects can be effectively and correctly authenticated. It is illustrated that the proposed method possesses high robustness against contaminations, and parameters (masks) flexibly designed at reference wave path can facilitate wavefront retrieval in the CCD plane and also can act like security keys. The proposed method provides a promising strategy for digital-holography-based optical security.

Acknowledgements

This work was supported by the National Natural Science Foundation of China (NSFC) (61605165), Hong Kong Research Grants Council Early Career Scheme (25201416), Shenzhen Science and Technology Innovation Commission through Basic Research Program (JCYJ20160531184426473), and The Hong Kong Polytechnic University (4-BCDY, G-YBVU, 4-ZZHM and 1-ZE5F).

References

[1] Schnars U, Jüptner W. Direct recording of holograms by a CCD target and numerical reconstruction. Appl Opt 1994;33:179–81.

[2] Schnars U. Direct phase determination in hologram interferometry with use of digitally recorded holograms. J Opt Soc Am A 1994;11:2011–5.

[3] Marquet P, Rappaz B, Magistretti PJ, Cuche E, Emery Y, Colomb T, Depeursinge C. Digital holographic microscopy: a noninvasive contrast imaging technique allowing quantitative visualization of living cells with subwavelength axial accuracy. Opt Lett 2005; 30:468–70.

[4] Javidi B. Securing information with optical technologies. Phys Today 1997;50:27–32.

[5] Yamaguchi I, Ida T, Yokota M, Yamashita K. Surface shape measurement by phase-shifting digital holography with a wavelength shift. Appl Opt 2006;45:7610–6.

[6] Takeda M, Ina H, Kobayashi S. Fourier-transform method of fringe-pattern analysis for computer-based topography and interferometry. J Opt Soc Am 1982;72:156–60.

[7] Yamaguchi I, Zhang T. Phase-shifting digital holography. Opt Lett 1997;22:1268–70.

[8] Awatsuji Y, Sasada M, Kubota T. Parallel quasi-phase-shifting digital holography. Appl Phys Lett 2004;85:1069–71.

[9] Tahara T, Ito K, Kakue T, Fujii M, Shimozato Y, Awatsuji Y, Nishio K, Ura S, Kubota T, Matoba O. Parallel phase-shifting digital holographic microscopy. Biomed Opt Express 2010;1:610–6.

[10] Cuche E, Marquet P, Depeursinge C. Spatial filtering for zero-order and twin-image elimination in digital off-axis holography. Appl Opt 2000;39:4070–5.

[11] Imbe M, Nomura T. Single-exposure phase-shifting digital holography using a random-complex-amplitude encoded reference wave. Appl Opt 2013;52:A161–6.

[12] Chen W, Chen X, Stern A, Javidi B. Phase-modulated optical system with sparse representation for information encoding and authentication. IEEE Photon J 2013;5: 6900113.

[13] Pérez-Cabré E, Cho M, Javidi B. Information authentication using photon-counting double-random-phase encrypted images. Opt Lett 2011;36:22–4.

[14] Yi F, Jeoung Y, Moon I. Three-dimensional image authentication scheme using sparse phase information in double random phase encoded integral imaging. Appl Opt 2017;56: 4381–7.
[15] Chen JX, Zhu ZL, Fu C, Yu H, Zhang LB. Gyrator transform based double random phase encoding with sparse representation for information authentication. Opt Laser Technol 2015;70:50–8.
[16] Pérez-Cabré E, Abril HC, Millan MS, Javidi B. Photon-counting double-random-phase encoding for secure image verification and retrieval. J Opt 2012;14:094001.
[17] Wu J, Haobogedewude B, Liu Z, Liu S. Optical secure image verification system based on ghost imaging. Opt Commun 2017;399:98–103.
[18] Fan D, Meng XF, Wang Y, Yang X, Pan X, Peng X, He WQ, Dong G, Chen H. Multiple-image authentication with a cascaded multilevel architecture based on amplitude field random sampling and phase information multiplexing. Appl Opt 2015;54:3204–15.
[19] Rajput SK, Kumar D, Nishchal NK. Photon counting imaging and phase mask multiplexing for multiple images authentication and digital hologram security. Appl Opt 2015;54:1657–66.
[20] Goodman JW, Introduction to Fourier Optics, 2nd ed. McGraw-Hill, 1996.
[21] Ozaktas HM, Zalevsky Z, Kutay MA. The Fractional Fourier Transform with Applications in Optics and Signal Processing, Wiley, 2001.
[22] Kreis T. Handbook of Holographic Interferometry: Optical and Digital Methods, Wiley-VCH, 2005.
[23] Javidi B. Nonlinear joint power spectrum based optical correlation. Appl Opt 1989;28: 2358–67.
[24] Chen W, Chen X. Grayscale object authentication based on ghost imaging using binary signals. EPL 2015;110:44002.
[25] Chen W, Chen X. Marked ghost imaging. Appl Phys Lett 2014;104:251109.
[26] Chen W, Javidi B, Chen X. Advances in optical security systems. Adv Opt Photon 2014;6:120–55.
[27] Chen W, Chen X. Object authentication in computational ghost imaging with the realizations less than 5% of Nyquist limit. Opt Lett 2013;38:546–8.
[28] Chen W, Chen X. Optical color-image verification using multiple-pinhole phase retrieval. J Opt 2014;16:075403.
[29] Wang X, Chen W, Mei S, Chen X. Optically secured information retrieval using two authenticated phase-only masks. Sci Rep 2015;5:15668.
[30] Chen W, Chen X. Digital holography-secured scheme using only binary phase or amplitude as ciphertext. Appl Opt 2016;55:6740–6.
[31] Chen W. Single-shot imaging without reference wave using binary intensity pattern for optically-secured-based correlation. IEEE Photon J 2016;8:6900209.
[32] Chen W. Multiple-wavelength double random phase encoding with CCD-plane sparse-phase multiplexing for optical information verification. Appl Opt 2015;54:10711–6.
[33] Chen W, Chen X. Ghost imaging for three-dimensional optical security. Appl Phys Lett 2013;103:221106.
[34] Chen W. Ghost identification based on single-pixel imaging in big data environment. Opt Express 2017;25:16509–16.
[35] Javidi B, Carnicer A, Yamaguchi M, Nomura T, Pérez-Cabré E, Millán MS, Nishchal NK, Torroba R, Barrera JF, He W, Peng X, Stern A, Rivenson Y, Alfalou A, Brosseau C,

Guo C, Sheridan JT, Situ G, Naruse M, Matsumoto T, Juvells I, Tajahuerce E, Lancis J, Chen W, Chen X, Pinkse PWH, Mosk AP, Markman A. Roadmap on optical security. J Opt 2016;18:083001.
[36] Chen W. 3D Gerchberg-Saxton optical correlation. IEEE Photon J 2018;10:7800409.
[37] Chen W. Virtually optical information verification with a hierarchical structure. Opt Eng 2018;57:010502.
[38] Shi Y, Li T, Wang Y, Gao Q, Zhang S, Li H. Optical image encryption via ptychography. Opt Lett 2013;38:1425–7.
[39] Chen LF, Chang G, He B, Mao H, Zhao DM. Optical image conversion and encryption by diffraction, phase retrieval algorithm and incoherent superposition. Opt Lasers Eng 2017;88: 221–32.
[40] Wang Q, Xiong D, Alfalou A, Brosseau C. Optical image authentication scheme using dual polarization decoding configuration. Opt Lasers Eng 2019;112:151–61.